

DTIC FILE COPY

2



Naval Research Laboratory

Washington, DC 20375-5000

NRL Memorandum Report 6382

AD-A207 035

# Review of Two Stream Amplifier Performance

P. M. PHILLIPS\*, E. G. ZAIMAN, H. P. FREUND\*  
A. K. GANGULY AND N. R. VANDERPLAATS

*Vacuum Electronics Branch  
Electronics Science and Technology Division*

*\*Science Applications International Corporation  
McLean, VA 22102*

March 23, 1989

DTIC  
ELECTE  
APR 20 1989  
S E D

Approved for public release; distribution unlimited.

089 4 20 034

SECURITY CLASSIFICATION OF THIS PAGE

REPORT DOCUMENTATION PAGE				Form Approved OMB No 0704 0188	
1a REPORT SECURITY CLASSIFICATION <b>UNCLASSIFIED</b>			1b RESTRICTIVE MARKINGS		
2a SECURITY CLASSIFICATION AUTHORITY			3 DISTRIBUTION/AVAILABILITY OF REPORT Approved for public release; distribution unlimited.		
2b DECLASSIFICATION/DOWNGRADING SCHEDULE					
4. PERFORMING ORGANIZATION REPORT NUMBER(S) NRL Memorandum Report 6382			5 MONITORING ORGANIZATION REPORT NUMBER(S)		
6a NAME OF PERFORMING ORGANIZATION Naval Research Laboratory		6b OFFICE SYMBOL (if applicable) Code 6840	7a NAME OF MONITORING ORGANIZATION		
6c. ADDRESS (City, State, and ZIP Code) Washington, DC 20375-5000			7b ADDRESS (City, State, and ZIP Code)		
8a. NAME OF FUNDING/SPONSORING ORGANIZATION		8b OFFICE SYMBOL (if applicable)	9 PROCUREMENT INSTRUMENT IDENTIFICATION NUMBER		
8c. ADDRESS (City, State, and ZIP Code)			10 SOURCE OF FUNDING NUMBERS		
			PROGRAM ELEMENT NO	PROJECT NO	TASK NO
			WORK UNIT ACCESSION NO		
11 TITLE (Include Security Classification) Review of Two Stream Amplifier Performance					
12 PERSONAL AUTHOR(S) Phillips,* P.M., Zaidman, E.G., Freund,* H.P., Ganguly, A.K. and Vanderplaats, N.R.					
13a. TYPE OF REPORT Interim		13b TIME COVERED FROM _____ TO _____		14 DATE OF REPORT (Year, Month, Day) 1989 March 23	15 PAGE COUNT 31
16 SUPPLEMENTARY NOTATION *Science Applications International Corp., McLean, VA 22102					
17 COSATI CODES			18 SUBJECT TERMS (Continue on reverse if necessary and identify by block number)		
FIELD	GROUP	SUB-GROUP	Two stream Amplifier		
19 ABSTRACT (Continue on reverse if necessary and identify by block number)					
<p>△ The basic concept of the two stream instability and its application to build a microwave/mm wave amplifier are reviewed from the perspective of the general usage of high frequency devices. A historical review of the relevant literature is presented with additional discussion of unpublished laboratory notebooks from the Naval Research Laboratory. A summary of the one-dimensional linear theory of the instability, along with the results from one-dimensional nonlinear particle simulation are given which are compared to other amplifier are discussed in comparison to other currently available devices that work in the same range of parameters. <i>CF</i></p>					
20 DISTRIBUTION/AVAILABILITY OF ABSTRACT <input checked="" type="checkbox"/> UNCLASSIFIED/UNLIMITED <input type="checkbox"/> SAME AS RPT <input type="checkbox"/> DTIC USERS			21 ABSTRACT SECURITY CLASSIFICATION <b>UNCLASSIFIED</b>		
22a NAME OF RESPONSIBLE INDIVIDUAL N.R. Vanderplaats			22a TELEPHONE (Include Area Code) (202) 767-3382	22c OFFICE SYMBOL Code 6840	

DD Form 1473, JUN 86

Previous editions are obsolete

SECURITY CLASSIFICATION OF THIS PAGE

S/N 0102-LF-014-6603

**CONTENTS**

I. INTRODUCTION AND HISTORICAL REVIEW ..... 1

II. LINEAR THEORY ..... 3

III. NONLINEAR ANALYSIS ..... 5

IV. SUMMARY AND DISCUSSIONS ..... 7

ACKNOWLEDGEMENT ..... 9

REFERENCES ..... 9

<b>Accession For</b>	
NTIS GRA&I	<input checked="" type="checkbox"/>
DTIC TAB	<input type="checkbox"/>
Unannounced	<input type="checkbox"/>
Justification	
By _____	
Distribution/	
<b>Availability Codes</b>	
Dist	Avail and/or Special
<b>A-1</b>	



# REVIEW OF TWO STREAM AMPLIFIER PERFORMANCE

## I. INTRODUCTION AND HISTORICAL REVIEW

In the past several years microwave/mm wave technology has advanced significantly due to new requirements for sensors and communications links. Microwave systems are better than optical and infrared systems for penetration of smokes, fog, dust and similar adverse environments. The advancement includes sources which provide high output power at higher frequencies and usually offer higher lifetimes and reliability. Applications of these systems cover wide areas, for example: communications, radar, radiometry, radio astronomy, spectroscopy, medical research and plasma diagnostics.

Short wavelength radar has some unique characteristics. For a given antenna size the beam width is smaller and the gain is higher than for radar at lower frequencies. High frequency radar also makes the atmospheric windows at 35, 94, 140 and 220 GHz accessible. Some applications require operation near one of the oxygen or water absorption bands, two of which are near 22.5 and 60 GHz. Short wavelength radar produces high spatial and frequency resolution which makes it extremely useful for estimating the radial velocity of a moving object. High spatial resolution results in high accuracy, which is necessary for acquisition of high resolution meteorological data at relatively short ranges. Finally, short wavelength radar can be operated at lower elevation angles without significant multipath and ground clutter interference.

Radiometric applications include remote sensing, navigation and imaging. In general, short wavelength systems are advantageous for communications applications because of their wide bandwidth and smaller antenna size.

We have reviewed the Two Stream Amplifier (TSA) as a candidate for a compact high power/short wavelength source that requires relatively low beam energies. The TSA is based upon the electron-electron two stream instability. For a strong interaction the two beams must be in close proximity to each other. This instability is known to be characterized both by an extremely high growth rate and an exceptionally broad bandwidth. For these reasons, interest in the TSA is longstanding. The project was considered by several groups during the period 1949-59. In 1949 Pierce and Hebenstreit<sup>1</sup> developed a one dimensional linear theory for a two stream amplifier and presented some normalized design curves. Their conceptual device is shown in Figure 1 and consisted of an input coupler (to inject a signal), a drift region for the electrostatic interaction, and an output coupler to convert the electrostatic energy into electromagnetic energy for extraction. The theory shows a very promising device with high gain and broad bandwidth that depends mainly on a velocity separation parameter  $b = 2(u_1 - u_2)/(u_1 + u_2)$  where  $u_1$  and  $u_2$  are the dc velocities of the two beams. Pierce<sup>2</sup> also discussed the effects of separation between the two beams on the gain, and considered the gap coupling for the input and output.

He introduced a coupling parameter  $S$  which varied from 0 (coincident beams) to 1 (uncoupled/infininitely remote beams). Some normalized design curves were given for various values of  $S$ .

Nergaard<sup>3</sup> presented a one dimensional mathematical model of a two beam tube. For a tube of 30 cm in length his model showed a gain of 120 dB at 3 GHz with a bandwidth of 0.9 GHz. Substitution of parametric numbers in his model shows that for realizable current densities ( $\leq 100 \text{ A}/(\text{cm})^2$ ) the ratio of two beam voltages can not be greater than 2. Since in a two stream interaction the slower beam gains energy at the expense of the faster one the maximum available output energy is at most this energy difference and this limits the efficiency of a TSA.

At Bell Laboratories, Hollenberg<sup>4</sup> performed an experiment using a helix as an input cavity, and tried both helix and gap output. He operated at 200 MHz and reported a gain of the order of 29 dB with a bandwidth of about 43%. The beam voltages were 54V and 33 V. The current in each beam was 1.1 mA. Maximum output power was 0.3 mW. For a gap output the maximum power obtained was 0.1 mW.

Haef<sup>5</sup> performed an experiment at NRL with a 3 GHz frequency and a total current of 15 mA using a helix as output coupler. He obtained a total gain of 46 dB. His publication shows details of the electron gun assembly and other experimental arrangements. Recently a considerable amount of data from these experiments has been recovered from old laboratory books at NRL (dated 1949-51). These experiments were performed by Haef<sup>6</sup> *et al.* The unpublished work includes a considerable amount of experimental data and device designs. A series of experiments were performed using coupled cavities as output and input coupling devices. The aim was to generate higher output power at the expense of the bandwidth. Figure 2 shows a drawing of the output end of the device. The length of the drift tube was varied from 6 inches to  $13\frac{1}{8}$  inches. Figure 3 indicates nomenclature for various parts of the tube. The resonator voltage ( $V_{k,r}$ ) was changed from 800 V to 3.5 kV keeping  $I_{k_1}$  and  $I_{k_2}$  fixed. The gain varied from 15 to 24 dBm and the results are shown in Figure 4. In order to increase the gain a new tube with a lower transit time was constructed. They also tried to operate the tube as a self excited oscillator and found 1.802 Watts of output power with  $(V_1 - V_2) = 335 \text{ V}$ . The voltage of resonator 1 was 2 kV and the currents were 100 mA and 150 mA. Figure 5 demonstrates the effect of velocity separation on the gain and the presence of an optimum value of this parameter. The best result was obtained using a tuning stub at the output. For a frequency of 3 GHz, collector current ( $I_{k_1} + I_{k_2}$ ) of 160 mA, beam voltages 1.12 kV and 1.59 kV, the output power was 6.3 Watts and the corresponding efficiency was 2.5%. Figure 6 represents a page of the old laboratory notebook from which the data is taken for this writeup.

In 1958 Bernashevskii *et al.*<sup>7</sup> published the result of an experiment that was carried out in the Institute of Radio Engineering and Electronics of the Academy of Sciences of the USSR. In their electron gun, a portion of the electrons of the faster stream was used to heat the cathode supplying the slower stream. It produced an intermixed beam and provided stable operation. Figure 7, taken from Bernashevskii, shows that for strong interaction (large  $K$ ) the two beams have to be very well mixed. Although the design details were not given, they used tapered helices of different lengths as input and output devices. The maximum gain was 46 dB at 3 GHz with voltages 1.55 kV and 1.1 kV and current density  $153 \text{ mA}/(\text{cm})^2$ , which gives an efficiency of 4.72%.

The basic small-signal theory and the intended experimental parameters are discussed in section II. In section III the results of a one dimensional particle simulation are presented. Section IV contains the detailed conclusions.

## II. LINEAR THEORY

The small signal theory for a TSA with two mixed beams but no outer conducting wall has been presented many times in the past<sup>1,2,3,5</sup> but a complete numerical solution for a three dimensional case with a surrounding conducting wall has, to our knowledge, never been done. A cylindrical waveguide of radius  $a$  with the dominant  $\text{TM}_{01}$  mode is considered (Figure 8). The co-propagating electron beams are assumed to be well-mixed with radius  $b$  and the direction of propagation is denoted by  $\hat{z}$ . Since it is customary to isolate the rf by terminators at the input and output boundaries, the interaction region is considered separately.

In region I ( $0 \leq r \leq b$ ) the fields can be written as (in S.I. units) :

$$\begin{aligned} E_{zI} &= AI_0(\Gamma r)e^{i(\omega t - \beta z)} \\ E_{rI} &= \frac{i\beta\Gamma}{\alpha^2} AI_1(\Gamma r)e^{i(\omega t - \beta z)} \\ H_{\phi I} &= \frac{i\omega\epsilon_0}{\alpha^2} \Gamma AI_1(\Gamma r)e^{i(\omega t - \beta z)} \end{aligned}$$

where  $I_0$  and  $I_1$  are the modified Bessel functions,  $\Gamma^2 = (\beta^2 - k^2)L = \alpha^2 L$  and  $k = \omega/c$ . For the two beam case chosen<sup>1</sup>,

$$L = 1 - \frac{W_1^2 B_1^2}{\gamma_1^{(0)3} (B_1 - Z)^2} - \frac{W_2^2 B_2^2}{\gamma_2^{(0)3} (B_2 - Z)^2}$$

with

$$\begin{aligned}
 W_j &= \frac{\omega_{pj}}{\omega} \\
 B_j &= \frac{\beta_j}{\beta_{0b}} \\
 \beta_{0b} &= \frac{1}{2}(\beta_{1b} + \beta_{2b}) \\
 Z &= \frac{\beta}{\beta_{0b}}
 \end{aligned}$$

where  $\omega_{pj}$  is the plasma frequency of the  $j^{\text{th}}$  beam ( $j = 1, 2$ ),  $\beta_{jb} = (\omega/u_j)$  is the propagation constant of the  $j^{\text{th}}$  beam and  $u_j$  is the d.c velocity of the  $j^{\text{th}}$  beam. The zero order relativistic factor is denoted by

$$\gamma_j^{(0)} = \frac{1}{\sqrt{1 - (u_j/c)^2}}$$

In region II ( $b < r \leq a$ ) the electromagnetic fields are:

$$\begin{aligned}
 E_{zII} &= [CI_0(\alpha r) + DK_0(\alpha r)]e^{i(\omega t - \beta z)} \\
 E_{rII} &= \frac{i\beta}{\alpha} [CI_1(\alpha r) - DK_1(\alpha r)]e^{i(\omega t - \beta z)} \\
 H_{\phi II} &= \frac{i\omega\epsilon_0}{\alpha} [CI_1(\alpha r) - DK_1(\alpha r)]e^{i(\omega t - \beta z)}
 \end{aligned}$$

The three independent boundary conditions are

$$\begin{aligned}
 E_{zII} &= 0 \quad \text{at } r = a \\
 E_{zI} &= E_{zII} \quad \text{at } r = b \\
 H_{\phi I} &= H_{\phi II} \quad \text{at } r = b
 \end{aligned}$$

Using these boundary conditions the dispersion relation for the system is:

$$\sqrt{L}I_1(\Gamma b) \left[ K_0(\alpha b) - I_0(\alpha b) \frac{K_0(\alpha a)}{I_0(\alpha a)} \right] + I_0(\Gamma b) \left[ K_1(\alpha b) + I_1(\alpha b) \frac{K_0(\alpha a)}{I_0(\alpha a)} \right] = 0$$

Note that as  $a \rightarrow \infty$ ,  $I_0(\alpha a) \rightarrow \infty$  and  $K_0(\alpha a) \rightarrow 0$ , the dispersion relation reduces to the well known one:

$$\sqrt{L}I_1(\Gamma b)K_0(\alpha b) + K_1(\alpha b)I_0(\Gamma b) = 0$$

Since the normalized design curves for the unbounded case can be found in Pierce<sup>1,2</sup>, we will present more quantitative graphs with some practically realizable parameters.

Based on the information found from the past works,<sup>3</sup> we have chosen the following parameters to study:

$$V_1 = 18\text{kV}$$

$$V_2 = 10\text{kV}$$

$$J_1 = J_2 = 80\text{A}/(\text{cm})^2$$

Figure 9 shows gain in dB/cm as a function of frequency for this limiting (*i.e.* one-dimensional) case as well as for various values of  $b$ . Curves (a), (b), (c), and (d) correspond to  $b = 0.025, 0.035, 0.05$  and  $0.075$  inches respectively and represent four practical values for the parameter  $b$ . The curve (e) represents the one dimensional case. In order to have  $80 \text{ A}/(\text{cm})^2$  current densities, the required currents are 1A, 2A, 4A and 9A respectively. The bandwidth as well as gain decrease rapidly as the beam radius decreases. In Figure 10 we see the effect of the outer conductor on the gain for a constant ratio of the conductor to the beam radii ( $a/b = 4$ ) for various values of the beam radius keeping the current density at  $80 \text{ A}/(\text{cm})^2$ . The effect of the conducting wall becomes prominent only when the beam radius is small. It can be shown that even for a small beam radius, the effect of the wall becomes small as the ratio ( $a/b$ ) increases (*i.e.*, as the outer conductor becomes remote). Figure 11 shows the effect of the voltage ratio  $V_1/V_2$  upon gain. For  $V_1 = 18 \text{ kV}$ , the voltage ratio was varied from 1.8 to 1.3 for  $b = 0.025 \text{ in}$ . The difference in gain becomes prominent as we go towards higher frequencies. Thus, the voltage ratio for an experiment should be chosen depending on the operating frequency. Figure 12 supports the fact that for the same voltage ratio, the gain and bandwidth increase with decrease in the value of the higher voltage. Although figures 11 and 12 show increase in gain and bandwidth with decrease in  $V_1/V_2$ , this trend does not continue for long. As  $V_1/V_2$  approaches unity, the gain drops off rapidly and figure 13 shows this along with the fact that for every frequency there is an optimum value of the voltage ratio  $V_1/V_2$  at which the gain is maximum.

### III. NONLINEAR ANALYSIS

It is well known that the linear theory of two stream instability offers high gain and broad bandwidth. Pierce's theory shows that the distance between the beams has to be very small (*i.e.*, they have to be intermixed) for a strong interaction, and this has been supported by the Russian experiment<sup>7</sup>. This requirement becomes more severe as the frequency increases from the microwave to the mm wave regime. However, linear theory does not give any quantitative information about the saturation and the output power/ efficiency. In order to gain further insight into the interaction, a nonlinear theory

is necessary. Filimonov<sup>8</sup> presented the results of a nonlinear theory and computation for a two beam electron tube. Although the effect of thermal spread was not clearly mentioned, it was related to the ratio of ac to dc velocity modulation which was about 66%.

To obtain additional insight into the nonlinear processes and saturation behavior of a TSA concept, a series of electrostatic, one-dimensional particle-in-cell simulations were done. Similar simulations have been done previously, for example by Birdsall<sup>9,10</sup> *et al.* The parameters used for the simulation presented herein are as follows:

$$J_1 = 80\text{A}/(\text{cm})^2$$

$$J_2 = 80\text{A}/(\text{cm})^2$$

$$V_1 = 18\text{kV}$$

$$V_2 = 10\text{kV}$$

$$f = \text{operating frequency} = 10\text{GHz}$$

An initial thermal velocity spread was considered with  $(u_{th}/u_2) = 0.01$ . The average plasma frequency  $= \bar{\omega}_p = \frac{1}{2}(\omega_{p1} + \omega_{p2}) = 1.54 \times 10^{10}$  rad/sec, and the Debye length was  $\lambda_D = 3.85 \times 10^{-3}$  cm. A periodic boundary condition was used and the system length was  $l = 3.942\text{cm} = 1024\lambda_D$ . Figures 14, 15, 16 and 17 show that the two stream interaction saturates quickly and although it produces a bunched beam, the quality of bunching is not very good in the sense that a large phase space area is filled. Figure 18 shows that at the driving frequency (10 GHz), the ratio of ac to dc current modulation is about 55%. This corresponds with the result obtained by Filimonov<sup>8</sup>. Another result for this parameter was obtained earlier by Rowe<sup>11</sup>. He used a simplified theory of the interaction based upon the analysis of space charge waves in a klystron (Beck<sup>12</sup>) and obtained an estimate of 88% for the maximum value of this ratio. The efficiency in klystron-like devices is related to the ratio of ac to dc electron velocity, and quite high efficiencies are found when this ratio approaches 60%. On this basis one would naively expect high efficiencies in TSA as well; however, the experimentally found efficiencies were always less than 5%.

In order to explain the low observed efficiencies we take note that the TSA operates as a prebuncher for the output helix stage. Thus, the device is essentially a helix TWT with enhanced bunching due to the two stream interaction. There is an optimum point at which the output helix should be located relative to the bunching caused by the TSA section. If the helix begins at a point further downstream, the interaction should be degraded because the beam will overbunch and thermalize due to the continuation of the nonlinear phase of the two stream interaction. In the event that the helix begins at a point prior to the optimum location, one must consider the TWTA in the presence of two electron

streams. In this case, Rowe's nonlinear theory of a TWTA with two cold beams shows that for Pierce's gain parameter  $C$  of approximately 0.1 (which is a practical maximum), the maximum output efficiency is about 5% with warm beams degrading the performance still further. The thermal effect is potentially disastrous even when the output stage is optimally located. In order to estimate the maximum thermal spread  $\Delta v$  that can be tolerated, we observe that if  $k\Delta v > |\omega - kv|$  then the assumption of a cold beam can no longer be made. This implies that the ratio of the velocity spread to the bulk velocity of the beams must be less than the ratio of the gain to the wavenumber for a cold beam. For a TWT the ratio of  $\text{Im}(k)$  to  $\text{Re}(k)$  is:

$$\frac{\text{Im}(k)}{\text{Re}(k)} = \frac{\sqrt{3}C}{2 + C}$$

Therefore, when  $C = 0.1$ , the maximum thermal spread that can be tolerated for a cold beam is  $\Delta v/v = 8.2\%$ . For the particular case studied, the aggregate of the two beams at the saturation point for the two stream interaction indicates that  $\Delta v/v$  is a substantial fraction of the initial velocity separation between the beams and was approximately 20%. Thus it can be concluded that a major difficulty in the design and operation of the TSA is thermal degradation of the beam. This is exacerbated by the fact that the TSA has a broad band character and a wide spectrum of waves is excited which will lead to an even more rapid thermalization of the beam.

#### IV. SUMMARY AND DISCUSSIONS

Since the TSA is inherently a high gain device, the length of the overall device can be expected to be shorter than that of a helix TWTA. However the output efficiency will be sensitive to the precise length also. Too long an interaction region will overbunch the beams, while too short an interaction region will underbunch the beams in comparison to a helix output stage.

The TSA is also a broad band device. However, the bandwidth of the configuration ultimately chosen would involve a helix output stage which limits the bandwidth of the overall device to that defined by the helix. Thus there seems to be no advantage to be gained in bandwidth by going to a TSA instead of a helix TWTA. The choice of a cavity coupler as an output stage might result in a higher output efficiency than a helix, but it would be limited to an application which involves a narrow bandwidth. In addition, the bandwidth will also be sensitive to the length of the TSA region, since the required optimum length will vary with the frequency.

Although the high gain of the TSA concept confers the advantage of being relatively less sensitive to thermal effects, the crucial limitation occurs due to the thermal spread of the bunched electron beams. This thermal spread is found to be comparable to the velocity difference between the two beams, which is a large number in itself. Thus, although the TSA interaction can tolerate a relatively large thermal spread, it will produce a bunched beam of relatively large thermal spread as well which will seriously degrade the efficiency of the output stage.

Most importantly, the TSA imposes a severe constraint on the electron gun design. The generation of two well mixed, high current density, cold beams is not a routine operation at this time.

An additional problem is that the helix output stage is separated from the TSA interaction region by a terminator which cuts off the electromagnetic modes from this region. However, the TSA interaction is electrostatic in nature, and will not terminate at the boundary to the helix output stage. Thus, the two stream interaction will continue simultaneously with the interaction of the bunched beams and the helix. This can be expected to result in a further increase in the thermal spread of the beams and a degradation of the efficiency.

Backward wave oscillation is a common problem associated with TWT's. A few possible ways to suppress the backward wave oscillations are the following: *i*) reduction of the beam diameter to reduce coupling to the  $n = -1$  harmonic, *ii*) addition of distributed loss at the beginning of the output section which can degrade the efficiency if it is located too close to the output, *iii*) use of shorter output stage so that the current is below the BWO starting current *iv*) velocity steps or tapering to desynchronize the backward wave interaction which is a useful technique, *v*) use of frequency selective loss which should work very well but it is very hard to achieve in practice. The problem of backward wave oscillations is also expected in a TSA since the output stage is a TWT. If the length of the output device is small enough, this problem will not arise. As discussed before, the output device should be introduced to the beam prior to the saturation point of the two stream interaction, and the beam that enters into the output device is not very tightly bunched. Even if we neglect the thermal spread completely, it seems clear that the output device must be long enough to support a travelling wave interaction to get reasonably good output power and efficiency. Thus, the TSA does not necessarily eliminate the problem of backward wave oscillations.

The general conclusions that can be reached concerning the TSA are that it is an inherently high gain but low efficiency device. In addition the TSA appears to present no unambiguous advantages over such competitive microwave sources such as the helix

TWTA.

### ACKNOWLEDGEMENT

The authors greatly acknowledge many helpful discussions with former NRL researcher Mr. H. Arnett and also to their colleagues Dr. S. Y. Park and Mr. R. Kyser.

### REFERENCES

1. J. R. Pierce and W. B. Hebenstreit. *Bell Sys. Tech. Jour.* **28**, pp. 33-51, January, 1948.
2. J. R. Pierce. *Proc. I. R. E.* **37**, pp. 980-985, September, 1949.
3. L. S. Nergaard. *RCA Rev.* **9**, pp. 585-601, December, 1948.
4. A. V. Hollenberg. *Bell. Sys. Tech. Jour.* **28**, pp. 52-58, January, 1949.
5. A. V. Haeff. *Proc. I. R. E.* **37**, pp. 4-10, January, 1949.
6. A. V. Haeff. *Unpublished Works.* 1949-51.
7. G. A. Bernashevskii, P. S. Voronov, T. I. Iziumova and Z. S. Chernov. *Radiotekh. Elektron.* **4**, pp. 165-172, October, 1959.
8. G. F. Filimonov. *Radiotekh. Elektron.* **4**, pp. 197-209, 1959.
9. C. K. Birdsall. *Ph.D. Dissertation.* Stanford University, Stanford Electronic Research Laboratory Report 36, June, 1951.
10. C. K. Birdsall, A. B. Langdon. *Plasma Physics via Computer Simulation.* McGraw Hill, New York, 1985.
11. J. E. Rowe. *Nonlinear Electron-Wave Interaction Phenomena.* Academic Press, 1965.
12. A. H. W. Beck. *Space-Charge Waves.* Pergamon Press, 1958.

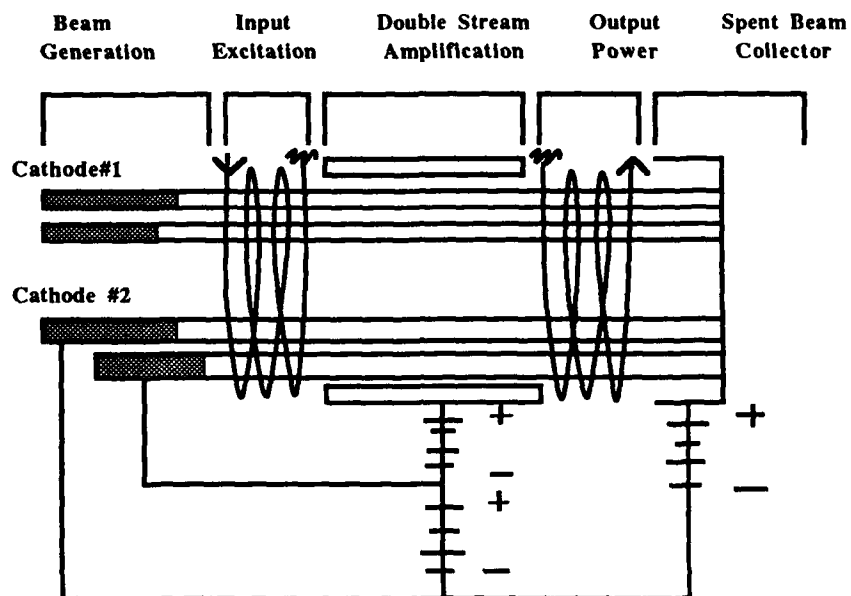


Figure 1. Two Stream Amplifier

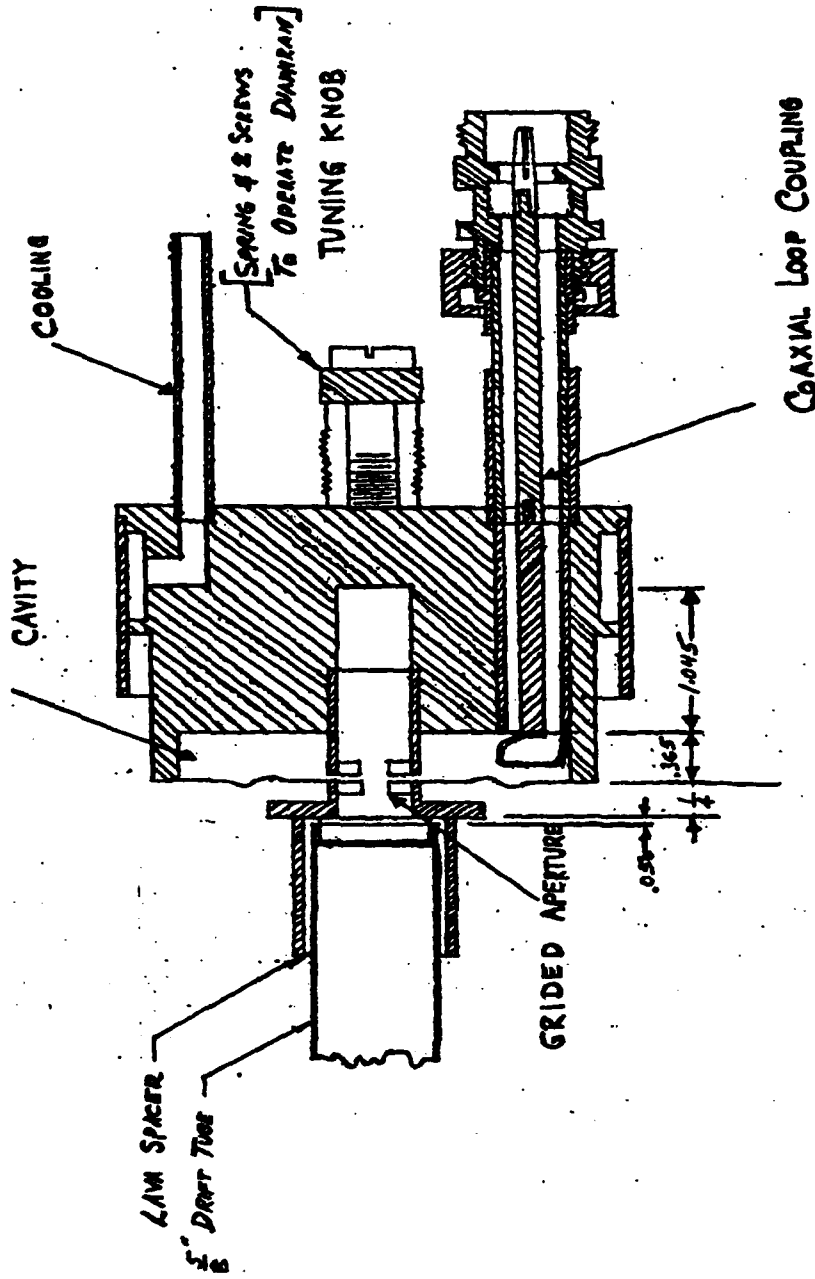


Figure 2. Output End of a Two Stream Amplifier (from a NRL logbook of 1949).

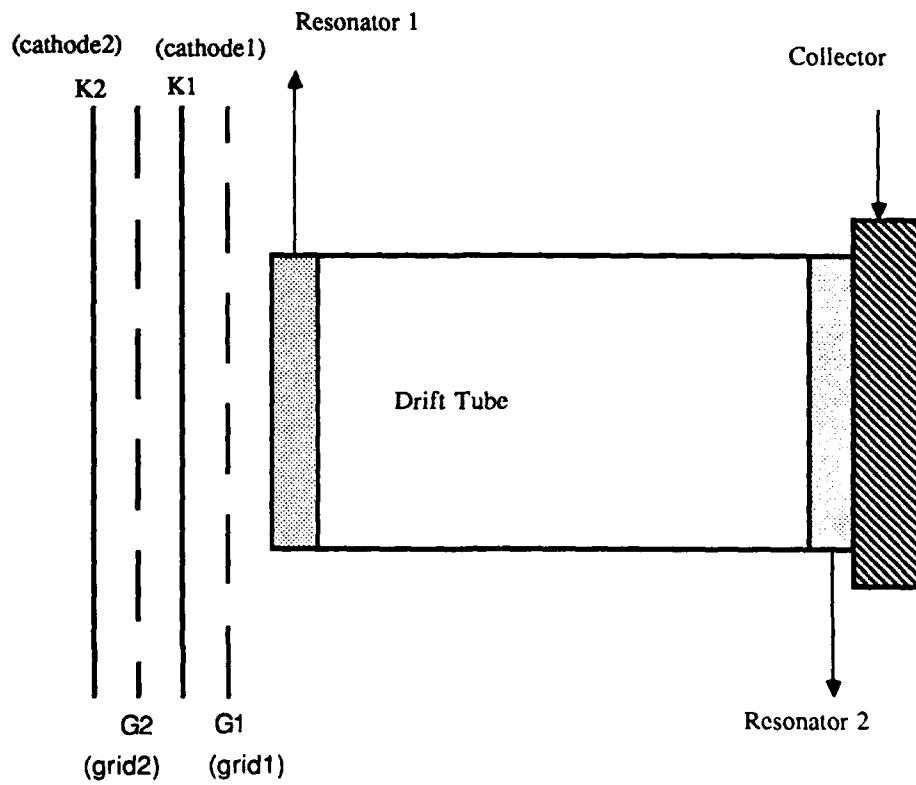
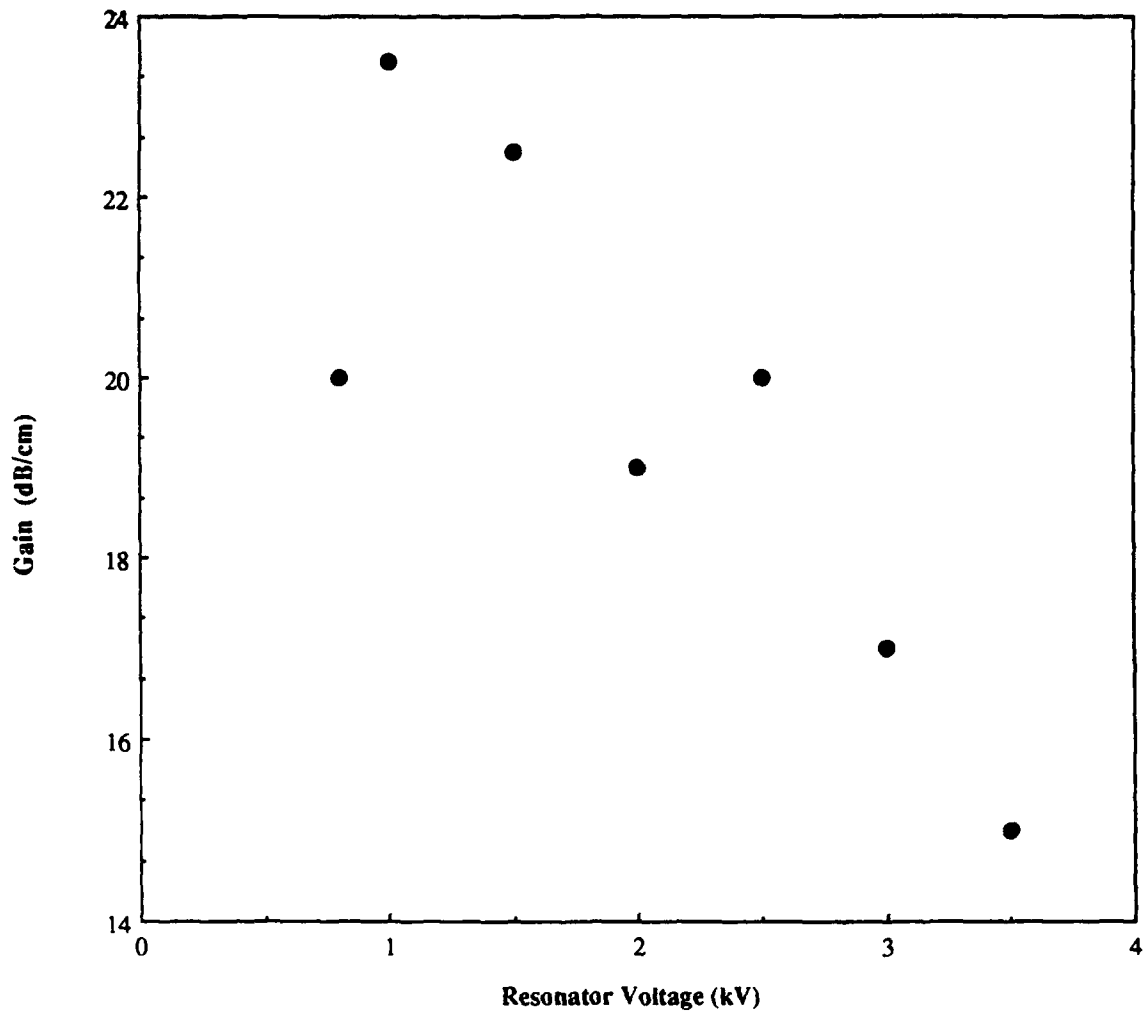
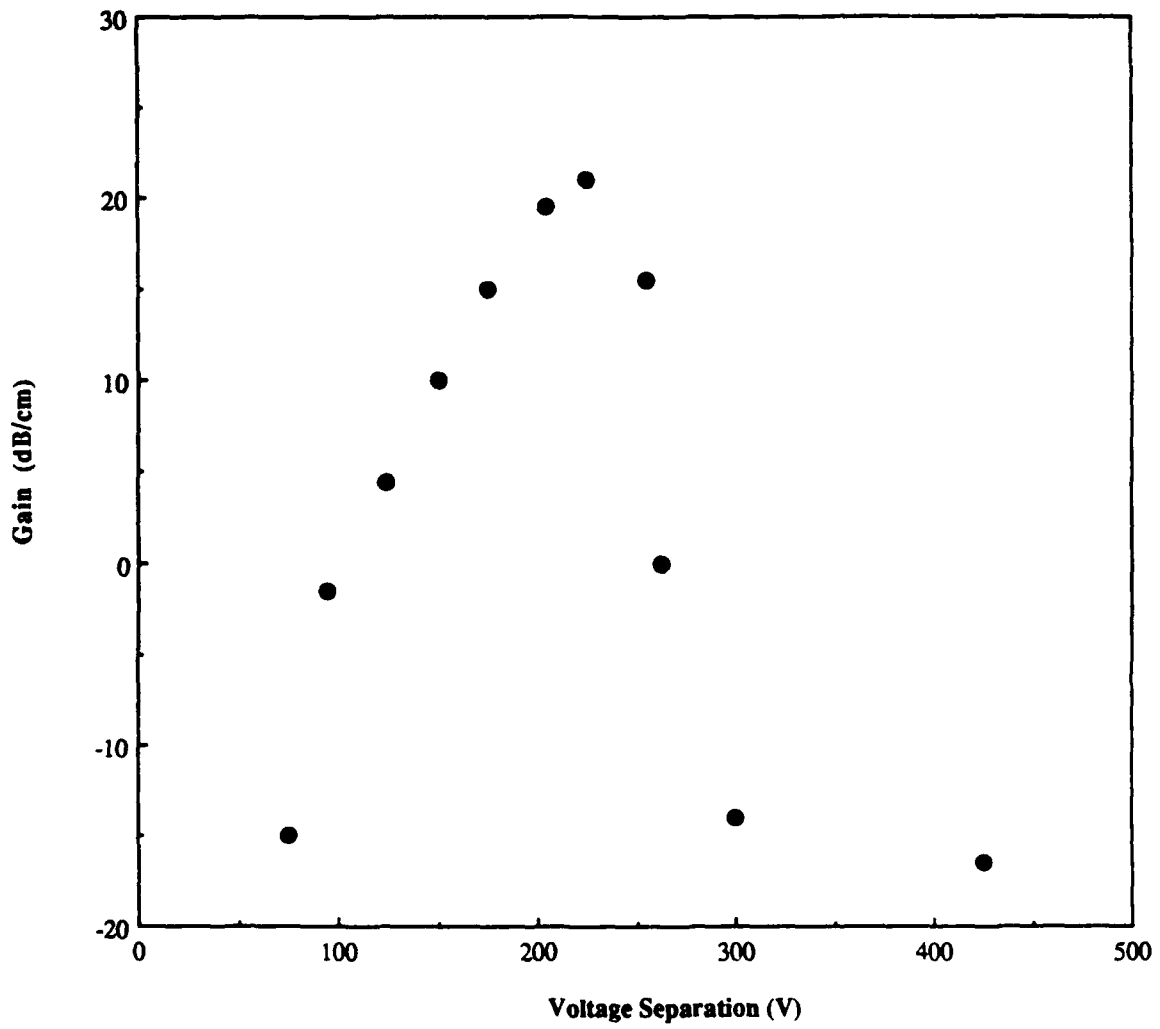


Figure 3. Nomenclature of the various parts of the "Electron Wave Tube", as used by Haeff et. al.

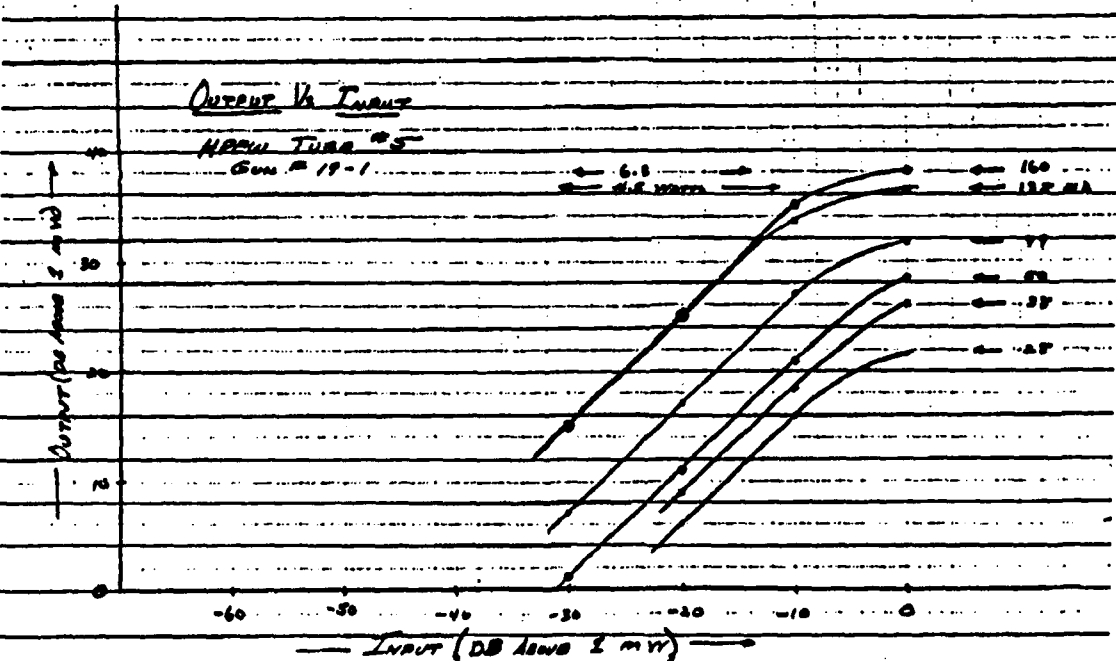


**Figure 4. Variation of Gain with the Resonator Voltage.  
Data taken from a laboratory note book of 1950.**



**Figure 5. Effect of Voltage Separation on the Gain.**  
V1 = 975 V, V2 = 800 V, I1 = 90 mA, I2 = 60 mA.  
Data taken from a laboratory notebook of 1949.

V <sub>g1</sub>	V <sub>g2</sub>	V <sub>g3</sub>	V <sub>g4</sub>	I <sub>g1</sub>	I <sub>g2</sub>	I <sub>g3</sub>	I <sub>g4</sub>	I <sub>g5</sub>	V <sub>g6</sub>	I <sub>g6</sub>	I <sub>g7</sub>	I <sub>g8</sub>	I <sub>g9</sub>	P <sub>in</sub>	P <sub>out</sub>
60	40	120	100	0	0	10	20	0	950	6.3	6.3	3	25	0	21.5
														-10	16
														-10	6
75	70	170	100	.5	0	15	30	0	950	6.3	6.3	3	25	0	26
														-10	17
														-10	9
90	100	200	100	.5	0	20	40	0	900	6.4	6.3	3	20	0	24
														-10	11
														-10	1
150	140	210	100	.5	.5	40	60	0	1300	6.4	6.4	3	29	0	24.5
														-10	2.7
														-10	1.7
														-10	7
220	215	410	1100	2.5	1.0	60	90	.5	1250	6.4	6.4	4.0	135	0	36.5
														-10	24.5
														-10	2.5
														-10	1.5
270	260	470	1130	4	1.0	90	90	.5	1500	6.6	6.3	4.0	160	0	37
														-10	2.5
														-10	2.5
														-10	1.5



Read and understood (obtain two signatures):  
 Witness \_\_\_\_\_ Date \_\_\_\_\_ Signature R.H. Lyman Date Dec 7, 1950  
 Witness \_\_\_\_\_ Date \_\_\_\_\_

Figure 6 . A page from a NRL logbook of 1950 showing the best results obtained by Haeff et al.

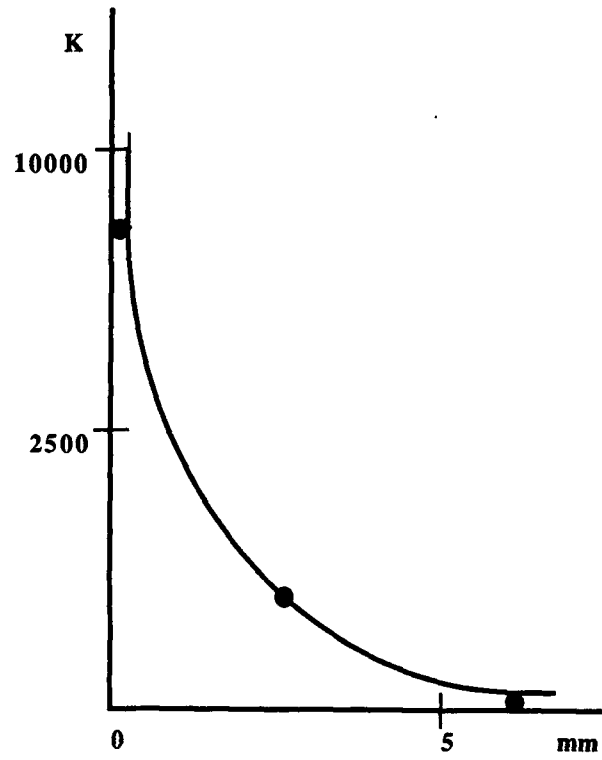


Figure 7. Effect of beam separation on the gain. Experimental points and theoretical curve are shown (taken from Bernashevskii).

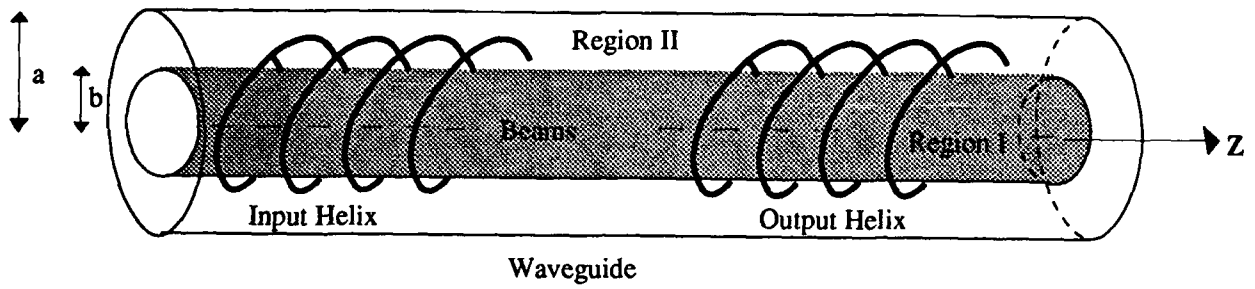


Figure 8. Basic Configuration.

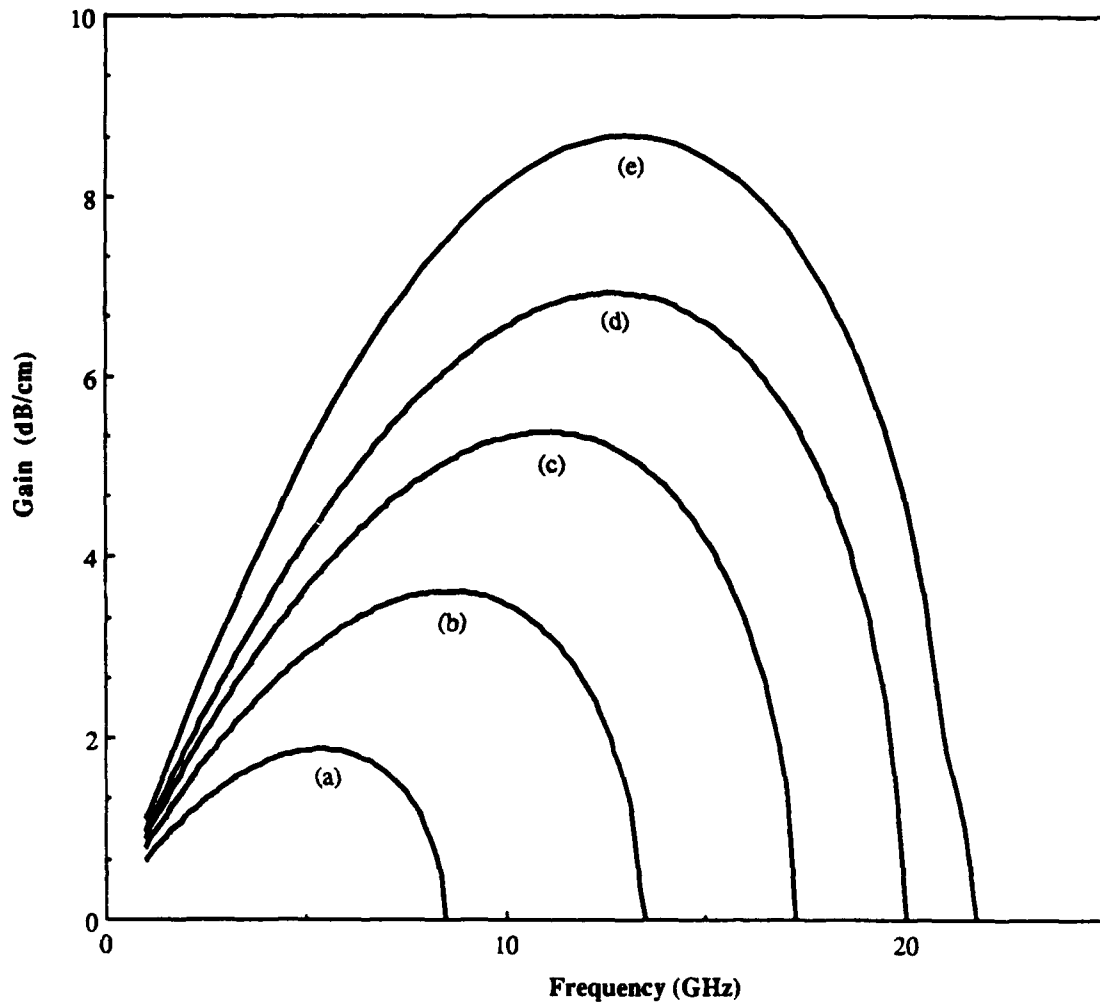


Figure 9. Gain vs Frequency for 1d Case (e) and for (a)  $b = .025$ ,  
(b)  $b = .035$ , (c)  $b = .05$ , (d)  $b = .075$  inches.

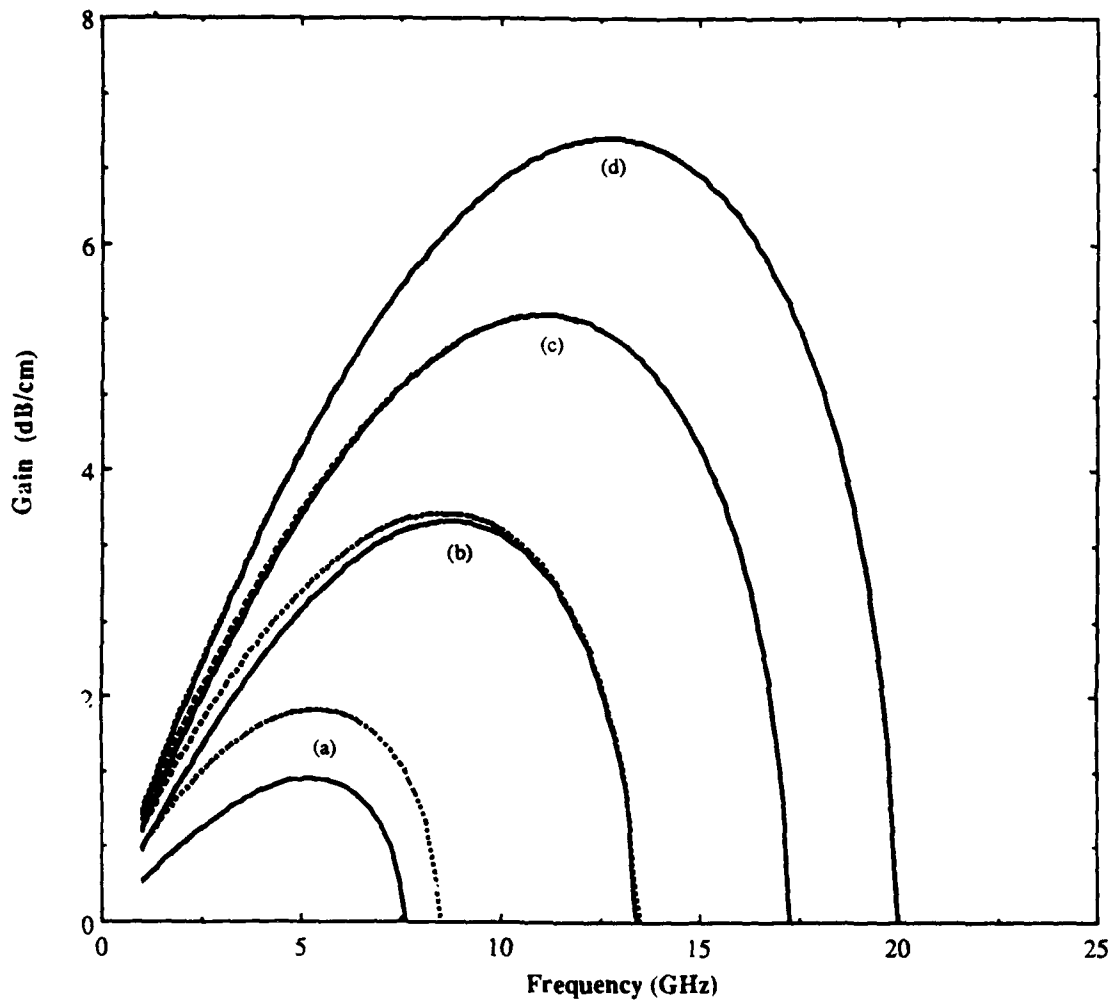


Figure 10. Effect of Outer Conductor on the Gain;  $a/b = 4$ ,  $V1 = 18$  kV,  $V2 = 10$  kV. Unbounded Case ....., Bounded Case —; (a)  $b = .025$  in, (b)  $b = .035$  in, (c)  $b = .050$  in, (d)  $b = .075$  in.

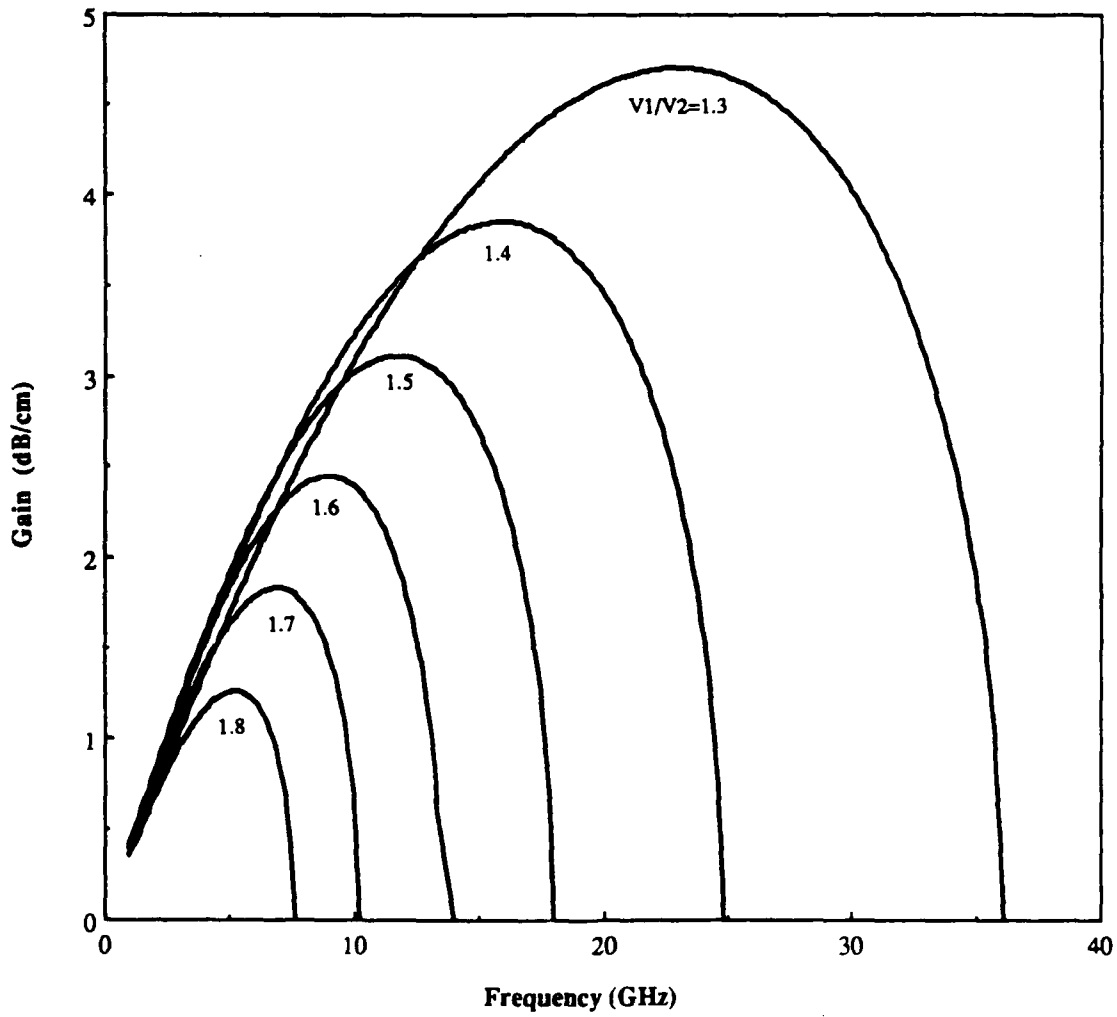


Figure 11. Effect of Voltage Ratio on the Gain;  $a/b = 4$ ,  $V_1 = 18$  kV,  $V_1/V_2 = 1.3, 1.4, 1.5, 1.6, 1.7$  and  $1.8$ .

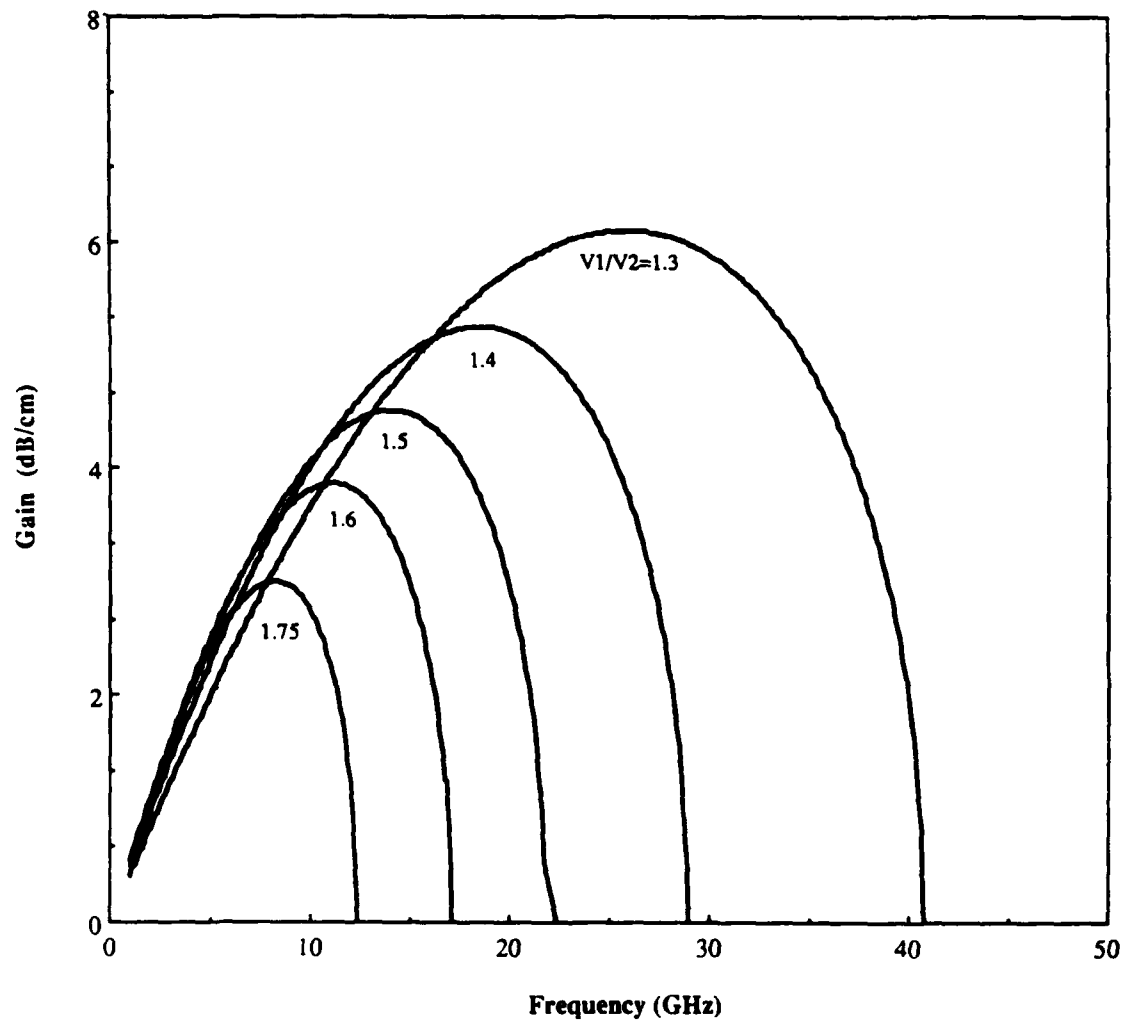
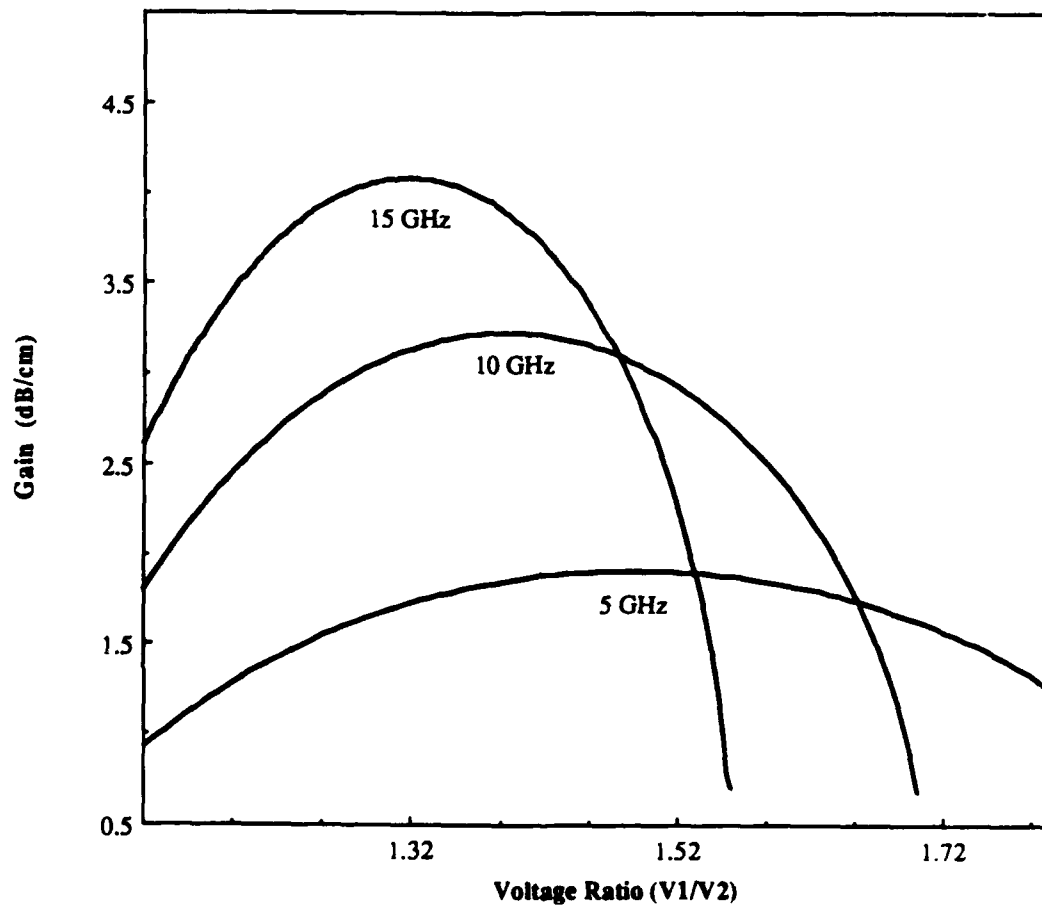
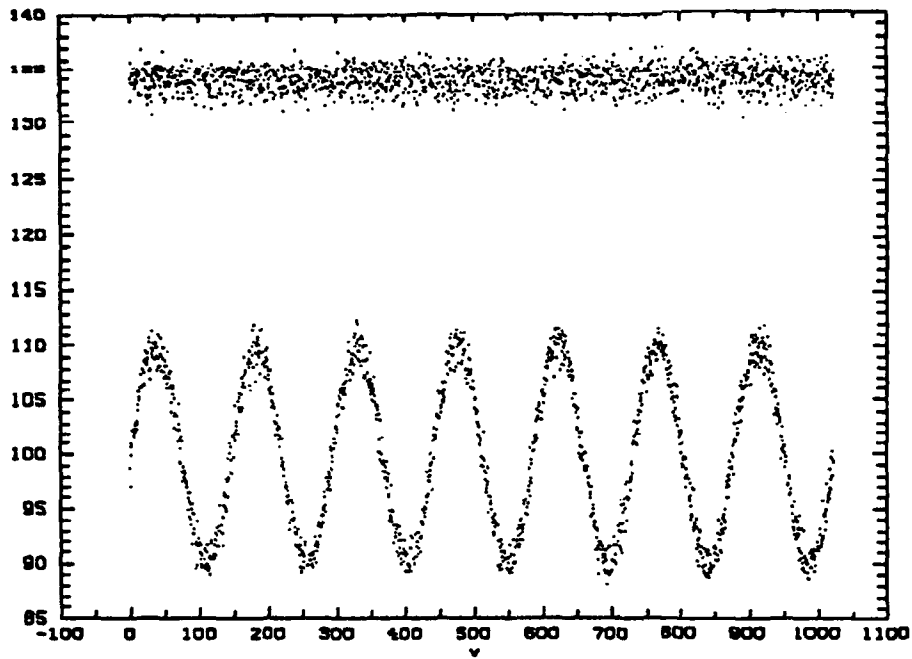


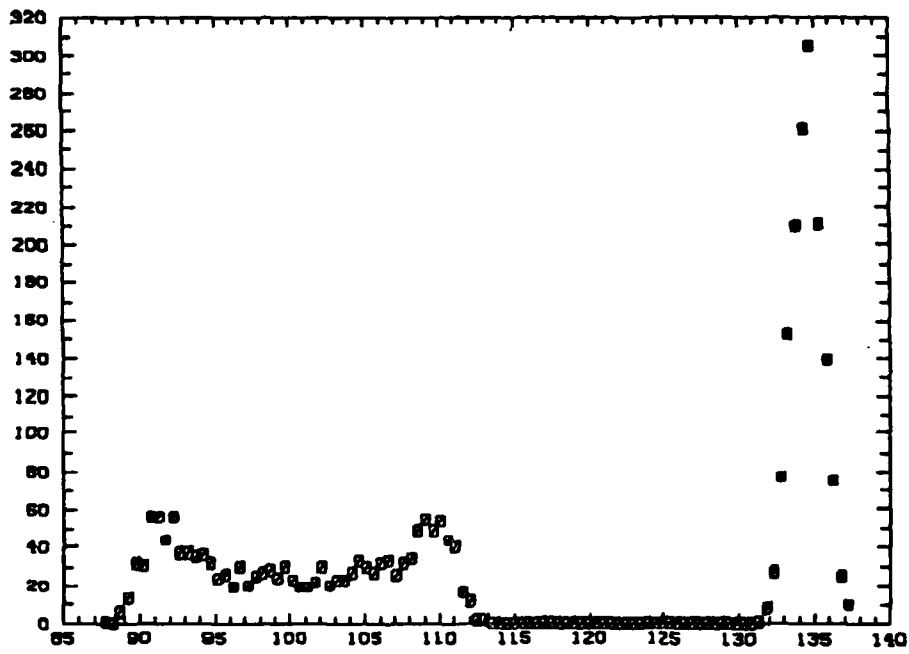
Figure 12. Effect of Voltage Ratio on the Gain for  $a/b = 4$ ,  $V_1 = 15$  kV, and  $V_1/V_2 = 1.3, 1.4, 1.5, 1.6, 1.75$ .



**Figure 13. For every frequency there is an optimum value of voltage ratio for which the gain is maximum.**

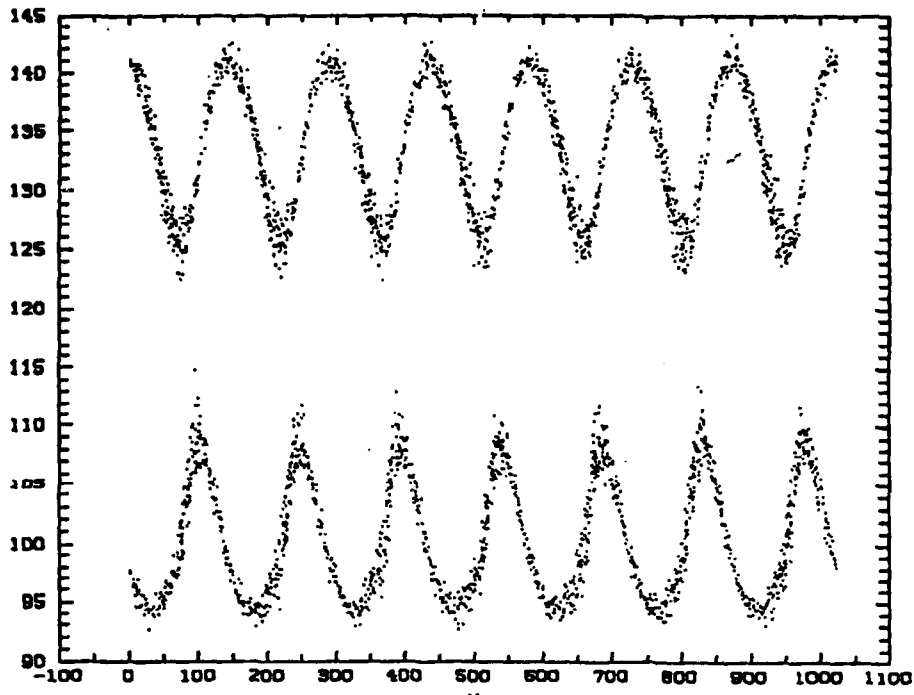


(a) Velocity -Position Phase Space



(b) Velocity Distribution Function.

Figure 14. At time = 0 both beams have the same thermal spread and the slower beam has the rf imposed.



(a) Velocity-Position Phase Space

(b) Velocity Distribution Function

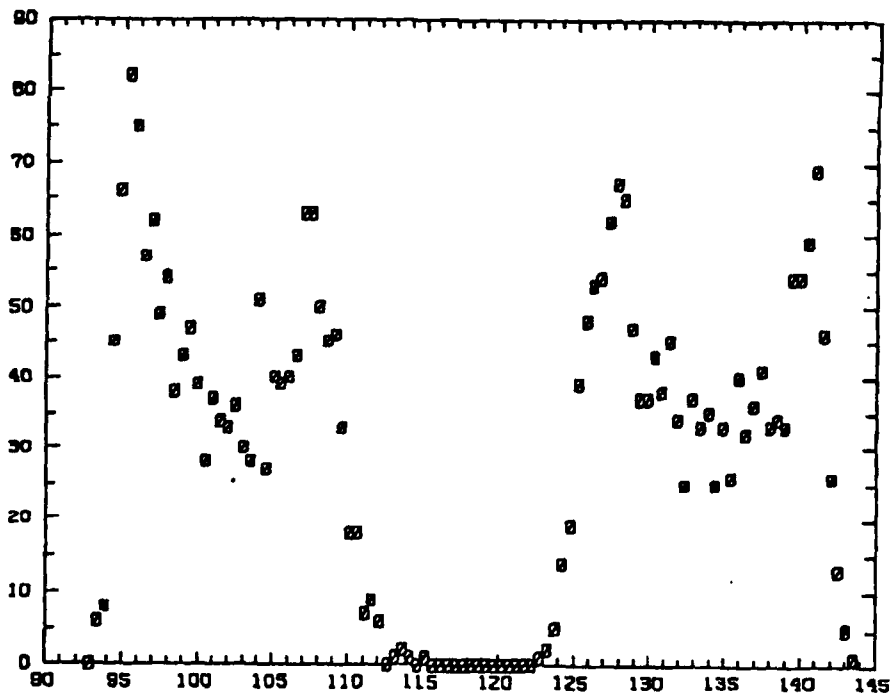
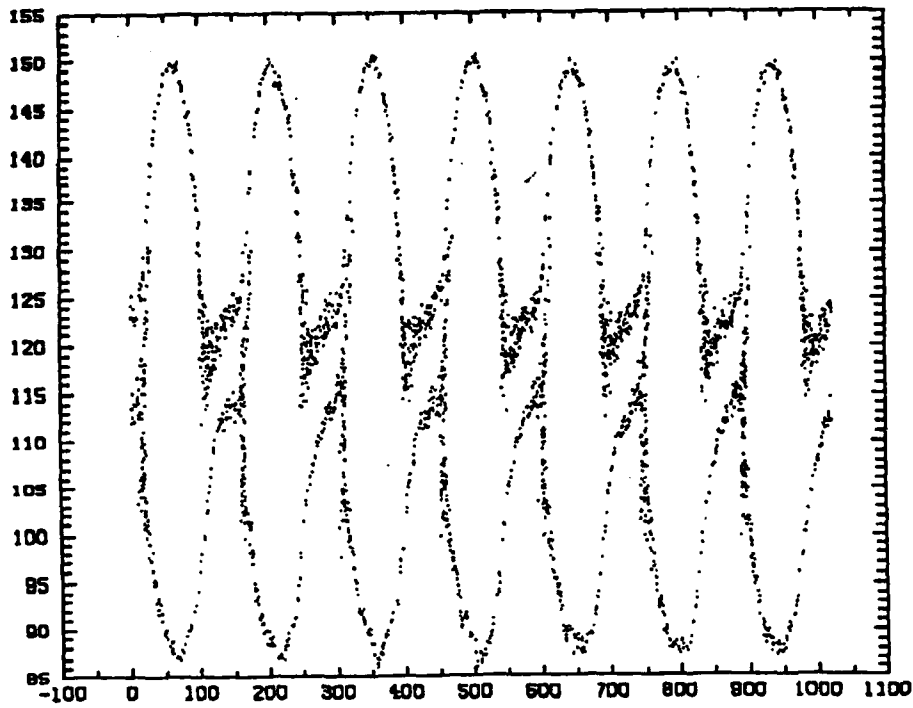


Figure 15. At time =  $3 \omega_p^{-1}$  the growth of the wave in the fast beam is shown.



(a) Velocity-Position Phase Space

(b) Velocity Distribution Function

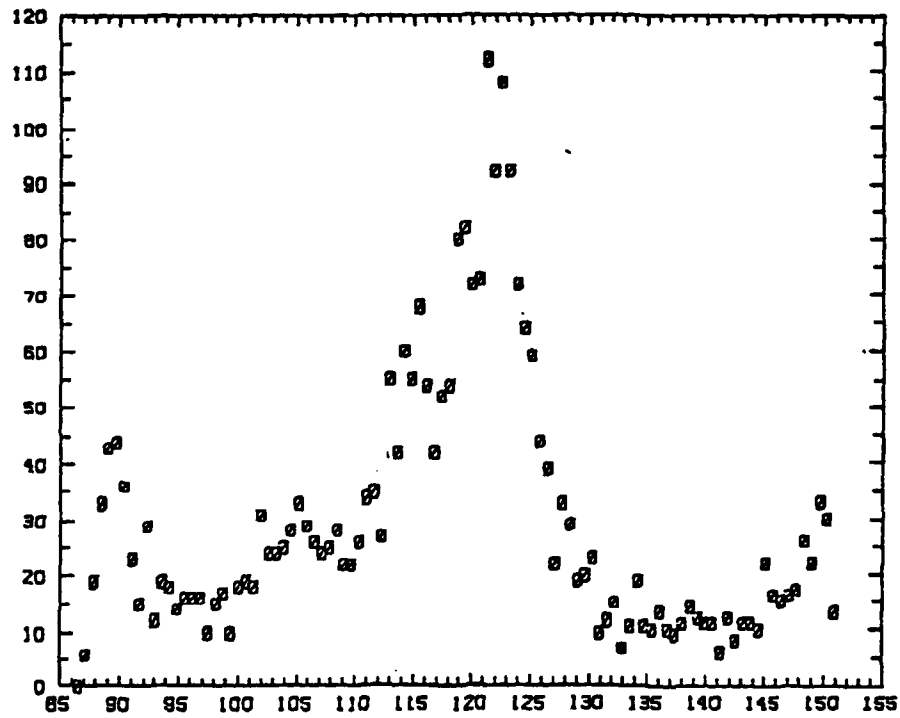
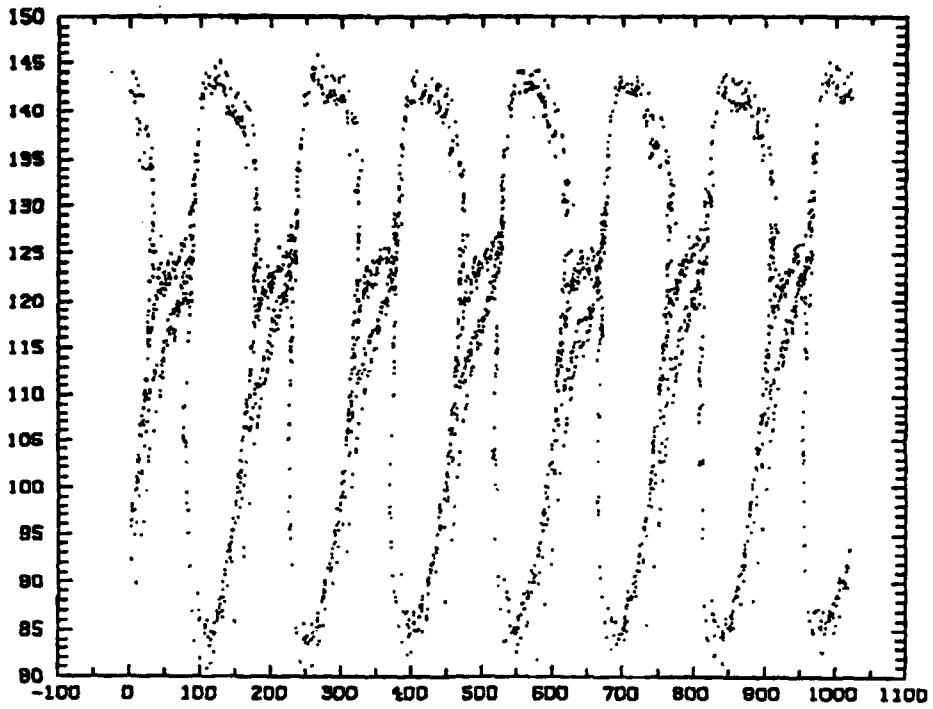


Figure 16. At time =  $6 \omega_p^{-1}$  the nonlinear beam-beam coupling and the thermalization of the distribution is illustrated.



(a) Velocity-Position Phase Space.

(b) Velocity Distribution Function.

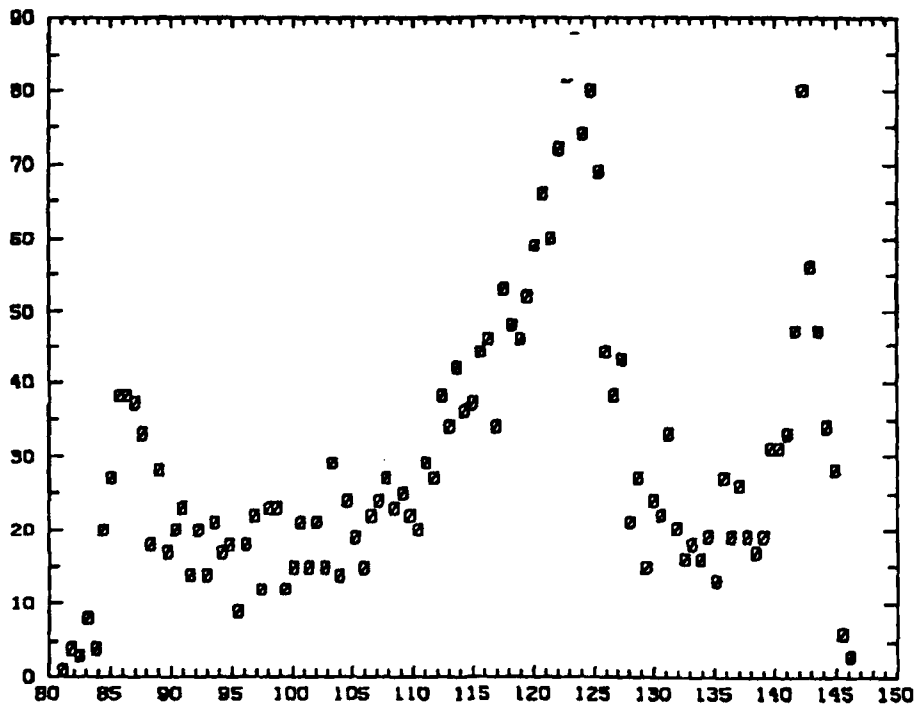


Figure 17. At time  $= 9 \omega_p^{-1}$  the continued nonlinear development of the system and the degradation in harmonic and thermal content of the system is shown.

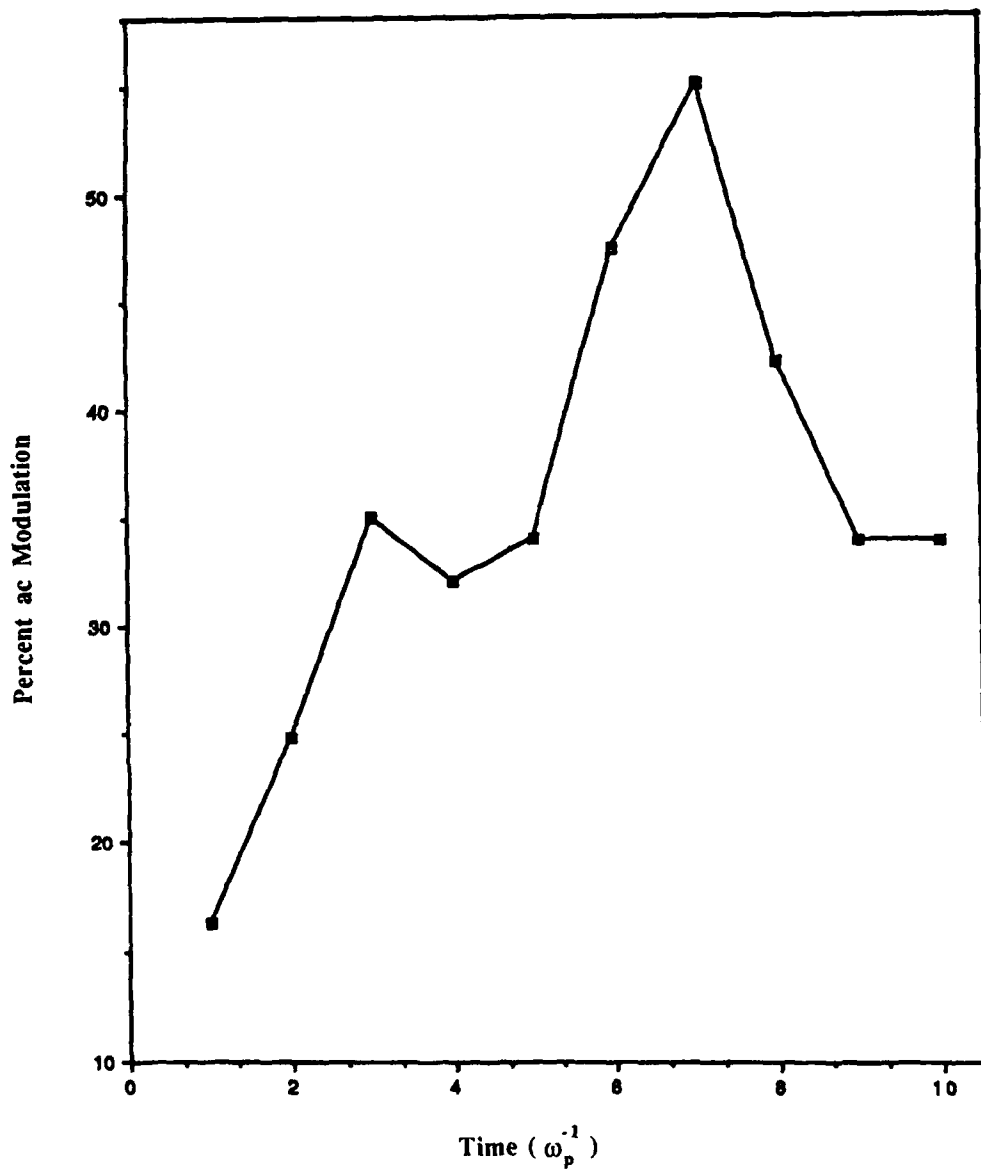


Figure 18. The percent ac modulation at the driving frequency (10 GHz) peaks near 55% when competing modes have grown to significance.